Numerical simulation of rock erosion performance of a high-speed water jet using an immersed body method

Xiang, J., Latham, J-P, and Pain, C.

Department of Earth Science and Engineering, Imperial College London, London, England, UK

ABSTRACT: The paper presents a new immersed body method (IBM) in which the combined Finite-Discrete Element Method (FEMDEM) that deals with solids interactions is coupled to other modelling technologies e.g. CFD, interface tracking, porous media etc. The CFD solver, Fluidity which is a general purpose multiphase CFD code is capable of modelling a wide range of fluid phenomena involving single and multiphase flows. The FEMDEM code, Solidity, can capture the deformation of the rocks, the initiation/propagation of new cracks. The immersed body method combined with adaptive mesh refinement has been applied to simulate the interaction between the high-speed water jet and rock mass. The paper aims to deeply understand the rock fragmentation mechanism and to explain the reasons for crack initiation, propagation and fragment removal under the impact load of a high-speed water jet. It also investigates the effect of pore water pressure on rock erosion performance. The results are in good agreement with experimental results.

1. INTRODUCTION

Over the past 20 years, radial water jet drilling (RJD) has been developed as a well stimulation technique which can enhance oil recovery. It can be used on existing wells to stimulate further extraction. RJD uses high-pressure water to be pumped through a high-pressure hose and a nozzle to drill into the rock. It erodes the rock by pumping a relatively small amount of water at high pressure and high velocity through a very small orifices of the nozzle.

Recently, the RJD technology has been considered as a stimulation technique for stimulating low performing geothermal wells. It is reported that, RJD stimulation was performed well in a low performing injection in Klaipeda, Lithuania in Europe, i.e. 12 laterals with a length up to 40m each were jetted using RJD technology, leading to an increase of injectivity of about 14% (Reinsch et al. 2018).

RJD has been claimed to be a less cost, more environmentally friendly alternative to hydraulic fracturing. However, there are some challenges and limitations to this technology. One of them is it cannot be used in all situations, e.g. static RJD is able to drill into sandstone, but difficult to deal with hard rock, like Icelandic Basalt. It is also found the rocks can be drilled into easier under ambient condition than true triaxial compression. After true triaxial compression is applied to

the rocks, the rate of penetration (ROP) of the rocks decreases significantly. The mechanisms of rock erosion are not fully understood.

In order to under the mechanisms of the rock erosion by RJD, there are several studies on investigating the interaction between a fluid and solid using numerical tools. Sakaguchi et al (2013) developed a three-dimensional Smoothed Particle Hydrodynamics (SPH) method code for the numerical simulation of interaction between soft rock with high speed water jet. Liu et al (2015) used a numerical method of coupled finite element method (FEM) with smoothed particle hydrodynamics (SPH) in which the model of rock was established using FEM and the model of the water jet was established using SPH. They investigated the effect of water jet diameter, jet angle and velocity of water jet on the efficiency of rock cracking, in which the mechanism of water jet impacting rock was showed through analysing the impact momentum and energy of rock, mean cutting depth and cutting width. In a similar paper (Jiang et al. 2014), the coupled SPH/FEM method was used to understand the rock fragmentation mechanism and understanding the mechanisms for crushing zone formation, crack initiation, and propagation under the impact load of water jet.

However, these studies have only considered the application of water jet to rock under ambient conditions.

In order to examine the state of stress of a subsurface area where RJD normally operates, the geomechanical conditions are necessarily needed. The pore pressure magnitude can affect the principal, effective stress, then the fracture initiation and propagation. Recently, an advanced loose coupling fluid solid model based on three meshes via IBM was developed by Vire´ et al. (2012, 2015). This model coupled a FEMDEM solid model and a finite element based fluid model. The three meshes are solid, fluid mesh and a novel thin shell mesh surrounding the solid surface. A coupling term is introduced into the shell mesh to complete the coupling process. Yang et al. (2016, 2017) further improved this model by introducing the fluid stress terms into the coupling term. The stress terms enable the model to capture some viscous behaviour in FSI numerical simulations.

The paper presents a new IBM in which FEMDEM (Munjiza, 2004, Xiang et al. 2009) that deals with solids interactions is coupled to other modelling technologies e.g. CFD, interface tracking, porous media etc. The CFD solver, Fluidity (Pain, et al. 2005, Pain et al. 2001) which is a general purpose multiphase CFD code is capable of modelling a wide range of fluid phenomena involving single and multiphase flows. The Fluidity project's history has led to a number of novel, advanced methods based upon adapting and moving anisotropic unstructured meshes, advanced combined finite element and control volume discretisation. The paper aims to deeply understand the rock fragmentation mechanism and to explain the reasons for crack initiation, propagation and fragment removal under the impact load of a high-speed water jet. It also investigates the effect of pore water pressure on rock erosion performance.

The remainder of this paper is organised as follows. Section 2 presents the governing fluid and solid equations. The experiment setup is presented in Section 3. results and discussions are in Section 4. We discuss the strength and weaknesses of this approach and draw conclusions in Section 5.

2. METHODOLOGY

The new immersed body method is used for simulating rock fragmentation mechanism of water jet drilling. Coupling between solids and fluids is realised using a three-mesh approach. One mesh (fluid mesh) is used across the whole solution domain on which the fluids equations are solved and the second mesh (solid mesh) contains a finite element representation of the solid (possibly fracturing and fragmenting) structures. The third mesh (thin shell mesh) acts as a numerical delta function in order to help apply the solid-fluid boundary conditions. Adaptive meshing (Piggott, et al. 2001, Yang, et al. 2006) resolves down onto the complex geometry of the solids at the level of detail necessary, hence addressing one of the main challenges – the accuracy of

the flow field near the solid surfaces and the capture of boundary layer effects. The forces and volume fraction from the FEMDEM structure model are mapped onto the fluids mesh using FEM mapping and updated hydraulic forces are returned to the explicit transient dynamic FEMDEM modelling of the solids. The IBM also couples implicit and explicit solvers, i.e. implicit CFD solver for water jet and explicit FEMDEM solver for solid mechanics. The details of IBM can be found in Yang et al. (2016, 2017)

2.1. Equations for solid dynamics

For the structural dynamics, FEMDEM is used in our model. It has the ability to compute the motions and stresses of any stiffness and shape. The dynamics of the solid model is given by [10]:

$$F_{ext} - F_{int} + F_c + F_p + F_d = M_s \frac{\partial u_s}{\partial t} \qquad (1)$$

where, F_{ext} and F_{int} denote the external and internal force, respectively, F_c is the contact force when collisions happen among multiple solids, M_s represents the mass, u_s is the solid velocity, t denotes the time, F_d and F_p are the exchange forces between the fluid flow and solids due to the fluid pressure and viscous terms.

2.2. Equations for fluid dynamics

'Fluidity-Multiphase' (Pain, et al. 2005, Pain et al. 2001), an open-source finite-element CFD model, is used here to model fluid flow. The continuity equation is:

$$\nabla \cdot u_f = 0 \qquad (2)$$

where u_f is the fluid velocity.

The momentum equation is given as follow:

$$\rho_f \frac{Du_f}{Dt} = -\nabla(p - \tau) + B_f + s_t \qquad (3)$$

where ρ_f is the fluid density, p denotes the fluid pressure, τ is the deviatoric stress tensor due to viscous effects, B_f represents the body force per unit mass (e.g. gravity), s_t is the coupling term, which gives out the effect of the solid motion on turbulent flow.

In order to embed the solid equations into the fluid equations, a supplementary equation connecting the solid and fluid velocities is given as follow:

$$\hat{\sigma}\left(u_s^s - u_f^s\right) = \hat{\sigma}\left(\hat{u}^f - u_f^f\right) \qquad (4)$$

where u^s_s and u^s_f represent the solid velocity on solid mesh and fluid velocity on solid mesh, respectively, u^f_f is the fluid velocity on fluid mesh, $\hat{\sigma} = \frac{\rho_f}{\Delta t}$, and $\hat{u}^f = \alpha_f u_f^f + \alpha_s u_s^f$, where α_s represent the fluid and solid volume fraction, respectively, Δt is the fluid time step. In this paper, the superscripts f and s refer the value on the fluid and solid mesh, respectively, and the subscripts f and

s represent the value of the fluid and solid, respectively. Thus, the continuity equation can be rewritten as:

$$\nabla \cdot \hat{u}^f = 0 ,$$

where:

$$\hat{u}^f = \begin{cases} u_s^f \text{ when } \alpha_f = 0, \alpha_s = 1 \\ u_f^f \text{ when } \alpha_f = 1, \alpha_s = 0 \end{cases} \quad (5)$$

2.3 Fracture model

The three-dimensional fracture model used in this paper was developed in the context of FEMDEM in the Dr Guo's PhD project (Guo, 2014). In his thesis, the cohesive zone fracture model (CZM) has been implemented. In the FEMDEM simulations, the entire domain is treated as a multi-body system and each discrete element is further discretised into a mesh of finite elements. The finite element formulation is used to simulate continuum behaviour for each discrete body, which includes the calculation of strain and stress in finite elements. The discrete element formulation is used to simulate discontinuum behaviour, e.g. contact interaction between discrete bodies and across discontinuities, which means the calculation of contact force and the distribution of contact force to finite element nodes. The fracture model links the finite element formulation with the discrete element formulation. For each intact discrete body, before fracture initiation, the stresses are calculated by the finite element formulation; if the stress state meets the failure criterion, a discrete fracture will form and then the interaction between discrete fracture surfaces will be modelled explicitly by the contact algorithms in the discrete element formulation; therefore, the whole process of transition from continuum to discontinuum can be realistically and accurately captured.

2.4 Pore pressure

The original formulation of Biot theory (Detournay and Chen, 1988) is used in this study, the total stress σ and the pore pressure p can be expressed as follows:

Total stress:

$$\sigma_{ij} = 2G\varepsilon_{ij} + \lambda\delta_{ij} - \alpha\delta_{ij}p \quad (6)$$

Pore pressure

$$p = -\frac{2GB(1 + v_u)}{3(1 - 2v_u)} + \frac{2GB^2(1 - 2v)(1 + v_u)^2}{9(v_u - v)(1 - 2v_u)}\zeta \quad (7)$$

Effective stress

$$\sigma'_{ij} = \sigma_{ij} + \alpha\delta_{ij}p \quad (8)$$

where δ_{ij} is the Kronecker delta, G is the shear modulus, v is the Poisson's ratio, v_u is the undrained Poisson's ratio, assuming $v_u = v/0.6$, B is Skemptons's pore pressure coefficient, α the Biot's coefficient.

In this study, it is assumed that the RJD rock breakdown process is under undrained conditions as pore water is unable to drain out of the rock in response to the impact of the water jet. This is reasonable as this paper focuses on what is breaking the rock under the very short time-scales of the transient behavior of jet-rock impact interaction. Consequently, the second term of the pore pressure equation can be ignored, and the pore pressure derived as follows

$$p = -\frac{2GB(1 + v_u)}{3(1 - 2v_u)}\varepsilon \quad (9)$$

$$\alpha = \frac{3(v_u - v)}{B(1 - 2v)(1 + v_u)} \quad (10)$$

3. MODEL SETUP AND MATERIAL PROPERTIES

The model setup is shown in Figure 1. The rock specimens are in the form of a slice with a diameter of about 50 mm and a thickness of 20 mm. Figure 1 shows a sketch of a rock specimen with dimension and target zones for the high-pressure water jet to act on. The standoff distance between rock surface and nozzle outlet is 6 mm and the diameter of orifice is 2mm. The exiting nozzle velocity magnitude varies from 0 m/s (nozzle wall) and 320 m/s (middle of nozzle), resulting in average velocity of 160 m/s (see Figure 2).
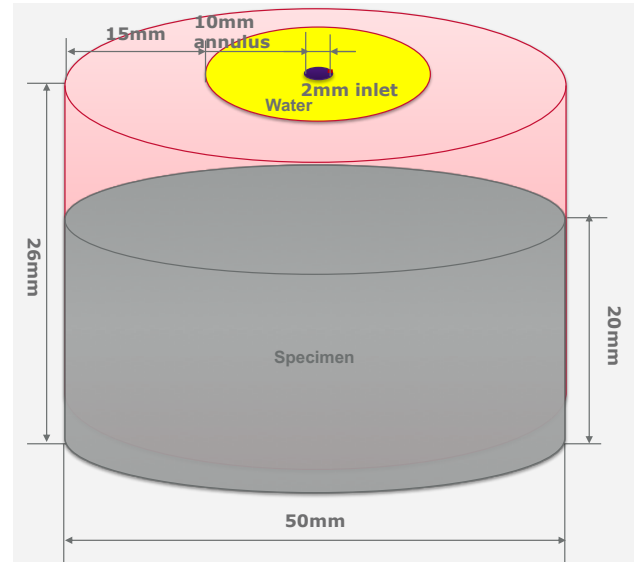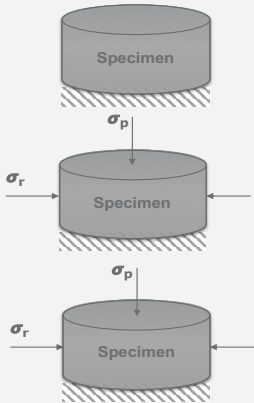

Figure 1 Sketch of simulation setup

Three rock types, Gildehaus sandstone, Dortmund sandstone, and Icelandic Basalt, are used in this study. The material properties of the rocks are measured in The Helmholtz Centre Potsdam - GFZ German Research Centre for Geosciences and listed in Table 1.

Table 2 shows the boundary conditions of the simulations, i.e. the bottom of specimen is fixed, and appropriate constraint conditions (such as pressures or stress confinement) can be applied to the remaining surfaces.

Table 1 material properties

	Gildenhaus	Dortmund	Icelandic Basalt
Young's modulus E GPa	19.5	21	17
Poisson's ratio v	0.265	0.12	0.22
Bulk Density (kg/m3)	2000	2425	2750
Tensile strength MPa	3.5	7.2	7.16
Internal friction angle	23	25	35
Cohesion MPa	17.5	22	38.5
UCS MPa	53	69	148
Gic J/m2	8.2	30.5	43.5
Giic J/m2	171.7	637.9	910.6

Table 2 boundary conditions

	Considering pore water pressure
	Atmospheric condition, bottom fixed
	σ_p=0.1MPa σ_r=5MPa bottom fixed
	σ_p=2.5MPa σ_r=5MPa bottom fixed

4. DISCUSSION

4.1 Mesh adaptivity

The simulation is computed based on an adaptive mesh which refines the mesh according to the proximity of the interface of the rock and the fluid velocity gradient, as shown in Figure 3. The minimum mesh edge size is 2×10^{-4} m and the maximum mesh edge size is 0.005m. The fluid mesh used by the fluid code in the coupling model is very refined near the fluid jet and vortices, and relatively coarse elsewhere.

4.2 Effect of rock strength

There are three rock types simulated in this paper: Gildehaus Sandstone, Dortmund sandstone, and Icelandic Basalt. Gildehaus Sandstone has the smallest tensile strength 3.5 MPa, and the lowest mode I & II energy release rates, 8.2 J/m^2 and 171.7 J/m^2 respectively. (see Table 1). As shown in Figure 4, only Gildehaus Sandstone can be eroded and cracked under water jet impact. The other two rocks have no fragment removal, although Dortmund Sandstone showed the stress state was near to inducing minor damage. This qualitatively agrees with experimental observations.

4.3 Effect of pore pressure

In this study, poro-elasticity is considered and Biot's theory has been implemented to simulate the effect of the water pore pressure. To understand the effect of the pore pressure, we reran the test shown in Figure 4a but considering the new pore pressure formulation. The new simulation results are shown in Figure 5b and compared with the previous results shown in Figure 5a. It is found that after considering pore pressure, RJD generates cracks in slightly wider areas. For this preliminary scenario considered, the result demonstrates that the pore pressure will act to enhance the RJD "jetability" but not significantly.

4.4 Effect of "water back pressure"

A water pressure head around the RJD nozzle, as distinct from the very high pressures impinging on the rock due to the jet, also called "back pressure", is needed to pump water from water chamber around RJD nozzle back to the surface. The effect of the back pressure has not been investigated in the past. In this paper, we consider the back pressure by adding it onto the fluid hydrostatic pressure. Some preliminary results are shown in Figure 6. When the back pressure is increased from 0.1 MPa to 2.5 MPa under the same constraint conditions (5 MPa on side wall surfaces), the rock ROP is significantly reduced.

5. CONCLUSIONS

This paper presents a new 3D immersed body method in which the fracture model was incorporated into a two-way fluid-solid coupling model. A methodology of using this model to capture hydraulic fluid-driven fracturing behaviour in high speed water jet drilling was proposed. To investigate the effect of the water pore pressure, Biot's theory was implemented. The effect of material mechanical strengths was also investigated.

The new fluid-solid coupling model with the fracture model is capable of simulating crack initiation, propagation and fragment removal under the impact load of a high-speed water jet. The numerical tests presented in this paper shows good agreement with experimental results qualitatively. It is worth mentioning that more quantitative benchmark tests, e.g. based on true triaxial compression, need to be done to validate this model. In future work, we will consider the effect of micro-structure on the interaction between high speed water jet and rock specimens as it is likely that the mechanisms important for an understanding of jetting action interact at a scale dominated by microstructure
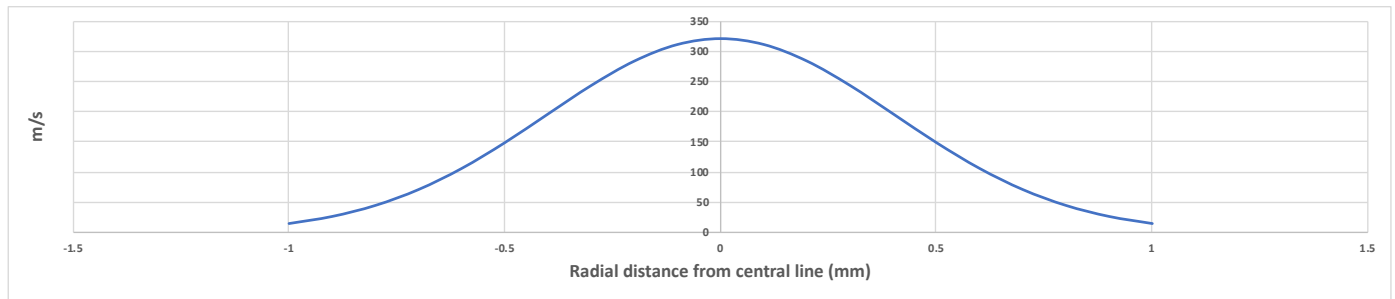
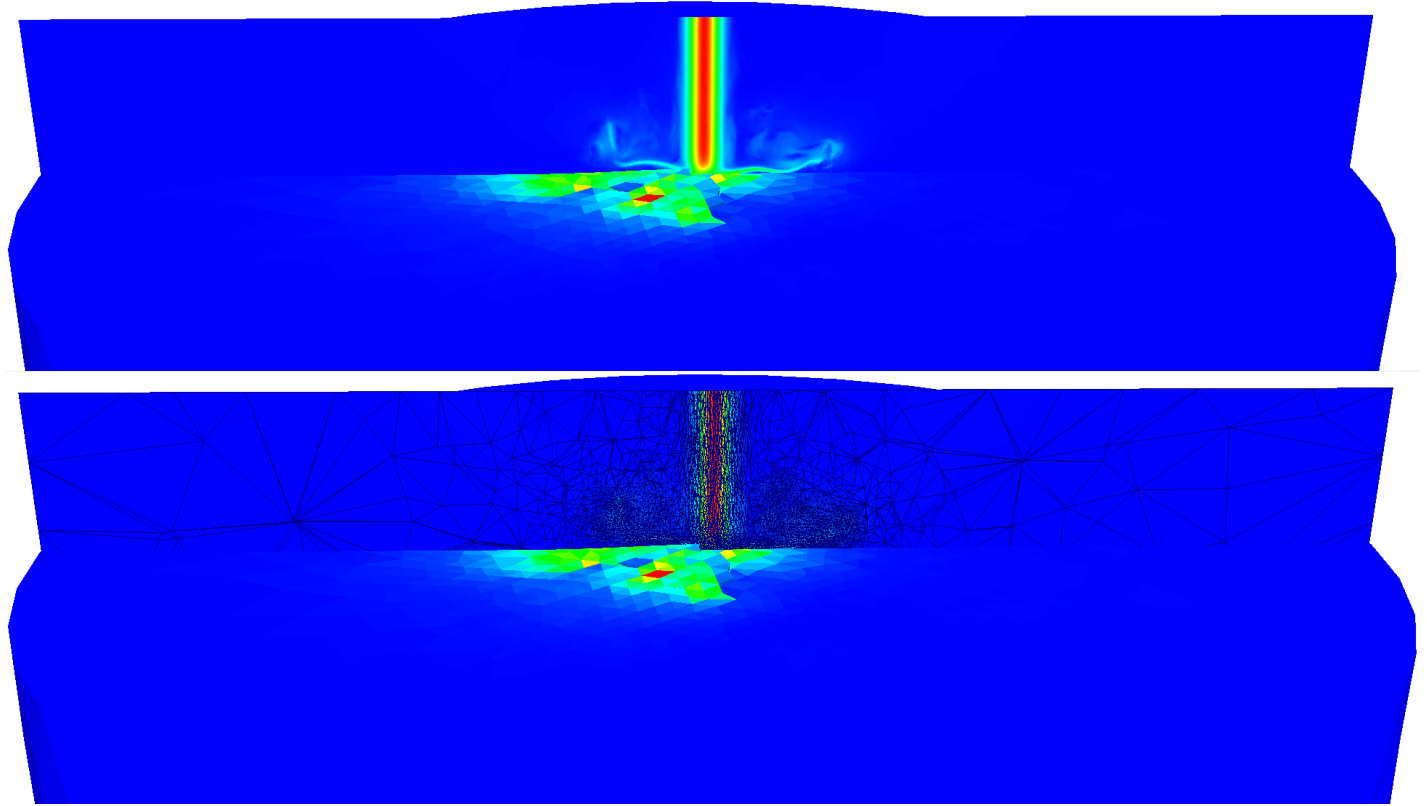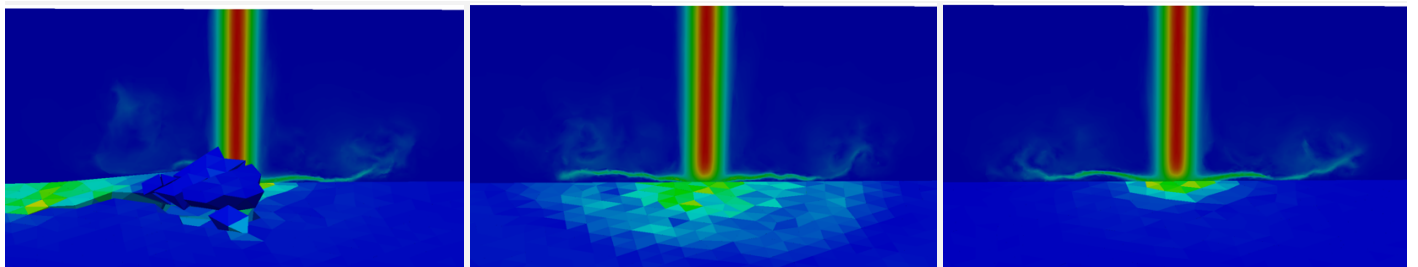Figure 2 exiting water velocity distribution

Figure 3. adaptive mesh refinement responding to water jet velocity

a) Gildehaus Sandstone   b) Dortmund sandstone   c) Icelandic Basalt

Figure 4 crack initiation and propagation responding to high speed jet drilling for different rock types: a) Gildehaus Sandstone; b) Dortmund sandstone; c) Icelandic Basalt

a)   b)
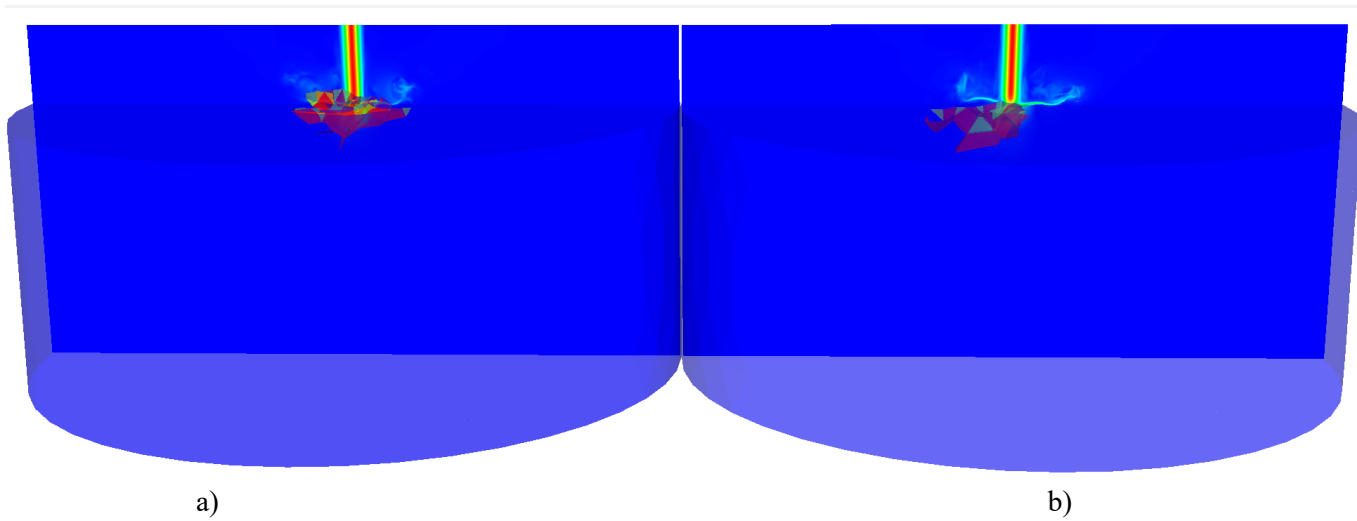
Figure 5 crack initiation and propagation responding to high speed jet drilling considering a) the effect of the pore pressure b) no effect of pore pressure
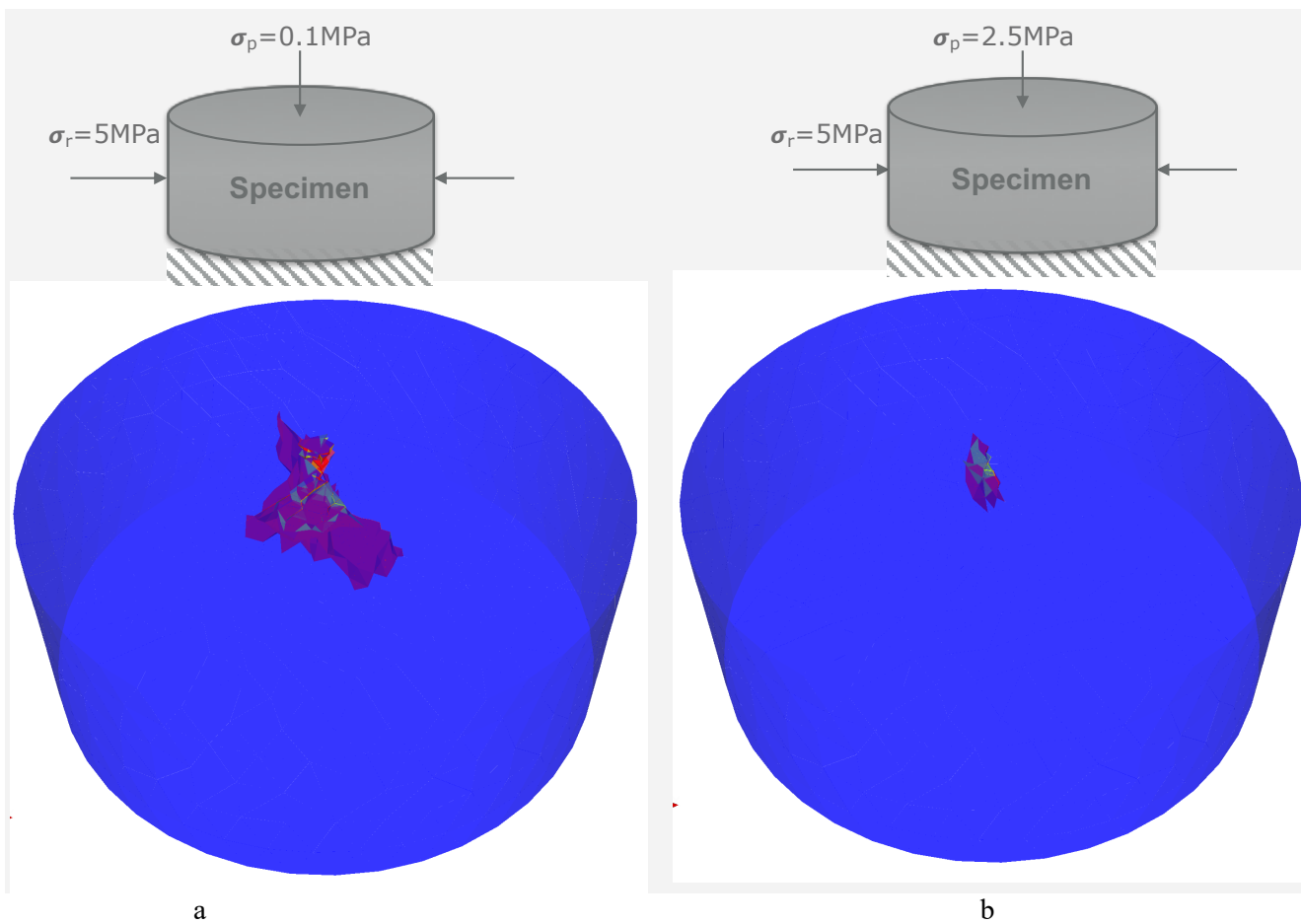

a   b

Figure 6 crack initiation and propagation responding to high speed jet drilling under back pressure of a) 0.1MPa, b) 2.5MPa

REFERENCES

1. Reinsch, T., B. Paap, S. Hahn, V. Wittig, and S. van den Berg, 2018, Insights Into the Radial Water Jet Drilling Technology - Application in a Quarry, Journal of Rock Mechanics and Geotechnical Engineering, Vol. 10(4)

2. Sakaguchi, K., Y. Yumoto, A. Kizaki, 2013, Numerical simulation of the water jet excavation of soft rock saturated with water, ISRM International Symposium - EUROCK 2013, 23-26 October, Wroclaw

3. Liu, X., S., Liu and H. Ji, 2015, Numerical research on rock breaking performance of water jet based on SPH, Powder Technology, Volume 286, December 2015, Pages 181-192)

4. Jiang, H., C. Du, S. Gao, K. Liu, 2014, Numerical simulation of rock fragmentation under the impact load of water jet, Shock and Vibration Volume 2014, Article ID 219489, 11 pages

5. Vire´, J. Xiang, F. Milthaler, P. E. Farrell, M. D. Piggott, J.-P. Latham, D. Pavlidis, and C. C. Pain, 2012, Modelling of fluid–solid interactions using an adaptive mesh fluid model coupled with a combined finite–discrete element model. Ocean Dynamics, 62(10-12):1487–1501, 2012.

6. Vire´, J. Xiang, and C. Pain, 2015, An immersed-shell method for modelling fluid– structure interactions. Philosophical Transactions of the Royal Society of London A: Mathematical, Physical and Engineering Sciences, 373(2035):20140085.

7. Yang, P., J. Xiang, M. Chen, F. Fang, D. Pavlidis, J.-P. Latham, and C. Pain, 2017, The immersed-body gas-solid interaction model for blast analysis in fractured solid media. International Journal of Rock Mechanics and Mining Sciences, 91:119– 132.

8. Yang, P., J. Xiang, F. Fang, D. Pavlidis, J.-P. Latham, and C. Pain, 2016, Modelling of fluid–structure interaction with multiphase viscous flows using an immersed body method. Journal of Computational Physics, 321:571–592.

9. Munjiza, A., 2004, The combined finite-discrete element method. John Wiley & Sons.

10. Xiang, J., A. Munjiza, and J.-P. Latham, 2009, Finite strain, finite rotation quadratic tetrahedral element for the combined finite–discrete element method. International Journal for Numerical Methods in Engineering, 79(8):946–978.

11. Pain, C., M. Piggott, A. Goddard, F. Fang, G. Gorman, D. Marshall, M. Eaton, P. Power, and C. De Oliveira, 2005, Three-dimensional unstructured mesh ocean modelling. Ocean Modelling, 10(1):5–33.

12. Pain, C., A. Umpleby, C. De Oliveira, and A. Goddard. 2001, Tetrahedral mesh optimisation and adaptivity for steady-state and transient finite element calculations. Computer Methods in Applied Mechanics and Engineering, 190(29):3771–3796.

13. Piggott, M., P. Farrell, C. Wilson, G. Gorman, and C. Pain, 2009, Anisotropic mesh adaptivity for multi-scale ocean modelling. Philosophical Transactions of the Royal Society of London A: Mathematical, Physical and Engineering Sciences, 367(1907):4591– 4611.

14. Yang, J. and E. Balaras., 2006, An embedded-boundary formulation for large-eddy simulation of turbulent flows interacting with moving boundaries. Journal of Computational Physics, 215(1):12–40.

15. Guo, L. 2014. Development of a three-dimensional fracture model for the combined finite-discrete element method. PhD thesis, Imperial College London.

16. Detournay, E., A.H.-D.Cheng, 1988, Poroelastic response of a borehole in a non-hydrostatic stress field, International Journal of Rock Mechanics and Mining Sciences & Geomechanics Abstracts, Volume 25, Issue 3, Pages 171-182